JOURNAL OF GEOPHYSICAL RESEARCH, VOL. 105, NO. A12, PAGES 27,767–27,776, DECEMBER 1, 2000

Ring current heating of the thermal electrons at solar maximum

M. W. Liemohn,[1] J. U. Kozyra,[1] P. G. Richards,[2] G. V. Khazanov,[3]
M. J. Buonsanto,[4,5] and V. K. Jordanova[6]

Abstract. To quantify the energy input to the thermal electrons due to Coulomb collisional degradation of hot ions in the inner magnetosphere, the heating rate is calculated from the results of a time-dependent kinetic ring current model. The large June 4-7, 1991, storm during the last solar maximum, when the hot O^+ content is maximal, is chosen for this study. Modeled electron heat fluxes into the topside ionosphere reach 10^{11} eV cm^{-2} s^{-1} on the dusk side, a large value that will certainly have an impact on the density, temperature, and composition of the upper ionosphere and thermosphere. Comparable maximum values of heat inputs to the inner magnetospheric thermal plasma are expected to arise again during storms of the present solar maximum. The calculated heating rates from the ring current simulations are compared directly with detailed ionospheric modeling results for the Millstone Hill field line ($L = 3$). It is seen that heating from the ring current is more than adequate to account for the nightside topside heat input necessary to obtain the observed electron temperatures during this storm, even taking into account the limitations of the comparison. The reason for this is the abundance of O^+ in the ring current at energies of a few tens of keV deep in the inner magnetosphere.

1. Introduction

The ring current is the current produced by energetic (1-300 keV) ions drifting around the Earth in the inner magnetosphere that are built up during geomagnetic disturbances. These particles are a major source of heat input to the thermal plasma in this region [*Kozyra et al.*, 1987, 1993, 1997; *Fok et al.*, 1995]. A primary energy deposition channel from the hot ions to the cool plasma is through Coulomb collisions. While both the thermal ions and electrons are heated by this population, the electrons are the most efficient at interacting with the ring current ions. Heating of the thermal electrons is achieved by ring current ions with speeds comparable to that of the thermal electrons. The maximum energy transfer per encounter occurs near 4 keV for H^+ and 50 keV for O^+ ions in a 1 eV thermal electron plasma [cf. *Kozyra et al.*, 1987]. Although the energy exchange is thought to occur near the equatorial plane, the high thermal conductivity of the electrons efficiently carries this energy along the magnetic field lines down into the topside ionosphere. Here the heated electrons interact with the neutral atmosphere, exciting certain species, particularly atomic oxygen, into metastable states and causing airglow emissions. When the emission is intense enough to exceed the sensitivity threshold of ground-based optical instruments, a stable auroral red (SAR) arc is identified (see reviews by *Rees and Roble* [1975], *Kozyra and Nagy* [1991], *Kozyra* [1992], and *Kozyra et al.* [1997]). In addition to SAR arc formation, effects of the storm time ring current on the thermal plasma are of vital importance for a completeness in global modeling efforts of the thermosphere, ionosphere, and plasmasphere, as well as for the understanding of large-scale remote sensing observations from the ground or from space. This is especially true during solar maximum, when the occurrence rate and intensity of geomagnetic storms increases over the solar minimum rate.

While several studies have quantified this heat input using global ring current models for storms at solar minimum [e.g., *Fok et al.*, 1993; *Jordanova et al.*, 1999], there has not been a comparable investigation for storms at solar maximum. Solar maximum is critical not only because we are now in the midst of one, but also because the composition and dynamics of the ring current are quite different at these times than at solar minimum. It has been shown in event studies that O^+ plays a critical role in energy deposition to the thermal electrons and thus SAR arc formation [*Kozyra et al.*, 1987; *Fok et al.*, 1991]. Inner plasma sheet populations that supply the storm time ring current attain a peak in O^+ concentration during solar maximum [*Young et al.*, 1982]. In fact, storms during this phase can produce ring currents that are dominated by O^+ [*Roeder et al.*, 1996; *Daglis*, 1997]. While the values of the magnetospheric heat input necessary to obtain a SAR arc have been quantified for solar maximum [e.g., *Kozyra et al.*, 1990; *Fok et al.*, 1991; *Lobzin and Pavlov*, 1999], the evolution and configuration of the ring current and plasmasphere that yield these values have not been investigated. A better understanding of these effects of the storm time ring current on the thermal plasma is necessary for rigorous global modeling efforts of the thermosphere, ionosphere, and plasmasphere, as well as for the interpretation of large-scale remote sensing observations from the ground or from space.

It is the goal of the present study to investigate the heating of the thermal electrons during the June 4-7, 1991, storm (during the last solar maximum). This was an intense storm with

[1]Space Physics Research Laboratory, University of Michigan, Ann Arbor.
[2]Computer Science Department, University of Alabama in Huntsville.
[3]Geophysical Institute and Department of Physics, University of Alaska Fairbanks.
[4]Haystack Observatory, Massachusetts Institute of Technology, Westford.
[5]Deceased November 1999.
[6]Space Science Center, University of New Hampshire, Durham.

Paper number 2000JA000088.
0148-0227/00/2000JA000088$09.00

an extended period of high activity. The *Dst* index, a prime indicator of storm and ring current strength, reached a minimum value of -230 nT (a large-magnitude storm). It is thought that the magnetopause crossed geosynchronous orbit several times for extended periods (several hours each time), and that dayside outflow was the major loss of ring current particles during the main phase of the storm [*Liemohn et al.*, 1999b]. This storm was chosen as an example of a major event during solar maximum and also because there have already been a large number of studies focusing on various aspects of this storm, such as solar/heliospheric [*Usmanov and Dryer*, 1995; *Smart and Shea*, 1995; *Mihalov and Strangeway*, 1995; *Ogunade*, 1997], magnetospheric [*Daglis et al.*, 1993; *Roeder et al.*, 1996; *Hudson et al.*, 1997; *Daglis*, 1997; *Burke et al.*, 1998; *Liemohn et al.*, 1999b], and ionospheric/thermospheric [*Smith et al.*, 1994; *Buonsanto*, 1995; *Salah et al.*, 1996; *Scali and Reinisch*, 1997; *Arriagada et al.*, 1998; *Pavlov et al.*, 1999] investigations. The present study examines the energy deposition rates from ring current ions into plasmaspheric populations and the aeronomic consequences. It is hoped that these results aid will not only in the understanding of geomagnetic storm effects but also in the planning and data analysis of geospace satellite missions.

2. Ring Current Energy Deposition Through Coulomb Collisions

When energetic plasma a is streaming through a background thermal plasma b, the energetic particles will lose energy to the thermal plasma through Coulomb collisions. The momentum transfer cross section σ_{ab}, considering the Debye shielding, is given as [*Bittencourt*, 1986]

$$\sigma_{ab}=4\pi\left(\frac{q_a q_b}{4\pi\varepsilon_o m^* g^2}\right)^2 \ln\Lambda , \tag{1}$$

where m^* is the reduced mass, g is the magnitude of the relative velocity, q_a and q_b are the charges of the hot and cold plasma particles, respectively, ε_o is the permittivity of free space, and ln Λ is the Coulomb logarithm. Assuming $v_a >> v_b$ ($g \sim v_a$), we have

$$\begin{aligned}
\sigma_{ii} &\sim \frac{e^4}{4\pi\varepsilon_o{}^2 E_i{}^2}\ln\Lambda , \\
\sigma_{ie} &\sim \frac{e^4}{16\pi\varepsilon_o{}^2 E_i{}^2}\left(\frac{m_i}{m_e}\right)^2 \ln\Lambda=\frac{1}{4}\left(\frac{m_i}{m_e}\right)^2 \sigma_{ii} , \\
\sigma_{ei} &\sim \frac{e^4}{16\pi\varepsilon_o{}^2 E_e{}^2}\ln\Lambda , \\
\sigma_{ee} &\sim \frac{e^4}{4\pi\varepsilon_o{}^2 E_e{}^2}\ln\Lambda=4\sigma_{ei} ,
\end{aligned} \tag{2}$$

where singly ionized plasmas are assumed and E_i and E_e are energies of ring current ions and electrons, respectively. It can be seen from (2) that most of the energy transferred to the plasmasphere from the ring current ions through Coulomb collisions goes to the thermal electrons. The mass ratio in σ_{ie} means that heavy ions (e.g., O^+) are the most efficient contributors to thermal electron heating among the ring current ion species. Furthermore, medium-energy (a few keV to tens of keV) ring current ions may have comparable velocity with the thermal (less than or equal to 1 eV) electrons. The small relative velocity between the two plasmas makes the energy transfer more efficient (g in (1)). In fact, the speed of a 1 eV electron equals that of a 4 keV H^+ ion and a 50 keV O^+ ion. As a result, medium-energy ring current ions, especially heavy ions, play an important role in the energy deposition to the plasmaspheric electrons. The study of *Kozyra et al.* [1987] showed that sufficient energy to power the SAR arcs observed on 2 selected days in 1981 is transferred to the electron gas at high altitudes via Coulomb collisions with ring current ions. In all cases, they found that O^+ was the major source of energy.

By integrating the Fokker-Planck collision term of Coulomb interactions a heating rate Q from a given ring current ion species a to a given thermal plasma species b can be derived,

$$\begin{aligned}
Q_{ab} &= -\int E\left(\frac{\delta f_a}{\delta t}\right)_{\text{coll}} d^3\mathrm{v} , \\
Q_{ab} &= \frac{e^4 \ln\Lambda\, n_b}{\varepsilon_o{}^2 T_b}\left[E\, G\left(\frac{\mathrm{v}_a}{\mathrm{v}_b}\right) j_a \Big|_{E_{\min}}^{E_{\max}} + \int_{E_{\max}}^{E_{\min}} G(\mathrm{v}_a/\mathrm{v}_b)\, j_a\, dE \right] ,
\end{aligned} \tag{3}$$

where j_a is the omnidirectional flux of ring current species a, E is the ring current particle energy, $E_{\min}$–$E_{\max}$ is the ring current energy range, n_b and T_b are the density and temperature of the background thermal plasma species b, and $G(x)$ is defined as

$$G(x)=\frac{\mathrm{erf}(x)-x\,\mathrm{erf}'(x)}{2x^2} . \tag{4}$$

Heat flux to the ionosphere P_{iono} can be obtained by integrating Q along the field line:

$$P_{\text{iono}}^b=\frac{B_i}{B_o}\int_0^{s_i} Q_{ab}\, ds , \tag{5}$$

where s goes from the equator ($s = 0$) to the ionosphere ($s = s_i$) and B_i and B_o are magnetic fields at the ionosphere and the equator, respectively. P_{iono} is the magnetospheric energy input to the ionosphere and is of interest for the energy deposition to the thermal electrons because thermal conduction down the field line is quite fast for these particles (that is, time delays for conduction down the field line will be neglected in this analysis). Note that this is an integral over only half of the field line, because the other half of the field line maps to the conjugate ionospheric foot point. Modeling studies have shown that the variations in P_{iono} have great effects on the thermal, compositional, and optical structures in the ionosphere [*Chandler et al.*, 1988; *Kozyra et al.*, 1990; *Fok et al.*, 1993].

This study concentrates on the ring current-thermal plasma interaction during a geomagnetic storm at solar maximum (June 4-7, 1991). Solar maximum is a good choice to examine this influence because of the high O^+ content in the storm time ring current (as opposed to H^+ dominance during solar minimum). *Roeder et al.* [1996] and *Daglis* [1997] found that a significant fraction (30-60%) of the ring current energy density during this storm is carried by O^+, on the basis of observations from the CRRES satellite, and *Liemohn et al.* [1999b] found up to a 70% *Dst** contribution from O^+ during the peak of this storm on the basis of the empirical formulas of *Young*

et al. [1982]. This is significant because O^+ is the major contributor to the energy deposition to both the thermal electrons and the thermal ions. Therefore more interaction is expected at solar maximum than at solar minimum.

In order to obtain the ring current fluxes for use in these equations a robust ring current model [*Fok et al.*, 1993; *Jordanova et al.*, 1996; *Liemohn et al.*, 1999b] will be used to simulate the ring current development and evolution during the chosen storm. This model solves the gyration and bounce-averaged kinetic equation [*Jordanova et al.*, 1996] by replacing each partial derivative with a conservative numerical finite-differencing scheme. The distribution function of a chosen ring current species is then time-dependently solved over a four-dimensional grid (in radial distance, local time, particle energy, and equatorial pitch angle). The model includes a source function from Los Alamos National Laboratory (LANL) geosynchronous orbit satellite measurements. Several loss mechanisms are also included, particularly Coulomb collision-induced scattering and energy degradation, charge exchange with the hydrogen geocorona, precipitative losses to the atmosphere, and outflow through the dayside boundary (located at geosynchronous orbit). The model also includes a magnetopause calculation following the formulation of *Shue et al.* [1998], and this magnetopause location is used as the outer boundary when it impinges on the simulation domain.

The observed and modeled *Dst** are shown in Figure 1a. This quantity is a measure of the magnetic field depression at the Earth's equatorial surface due to the ring current. Shown in Figure 1b is the *Kp* index during this storm, which maintained a high level ($Kp > 5$) for two straight days. The observed *Dst** value is found from the total Kyoto *Dst* value, followed by a removal of both the Earth's diamagnetic effect, which is just a division by 1.5 [*Dessler and Parker*, 1959], and the magnetopause currents, which are proportional to the solar wind dynamic pressure [*Burton et al.*, 1975]. The model results are found using the relation of *Dessler and Parker* [1959] and *Sckopke* [1966], which relates *Dst** to the total ring current energy. It can be seen that the model prediction of *Dst** follows the observed value through most of the storm. While several excursions exist, usually during times when there were no LANL measurements on the nightside for an accurate boundary condition, the trends are well matched, including the peak intensity value and the early and late period recovery rates. An analysis of these recovery rates was discussed by *Liemohn et al.* [1999b] and will not be discussed further here. This study will use results from this simulation to calculate heating rates to the thermal plasma.

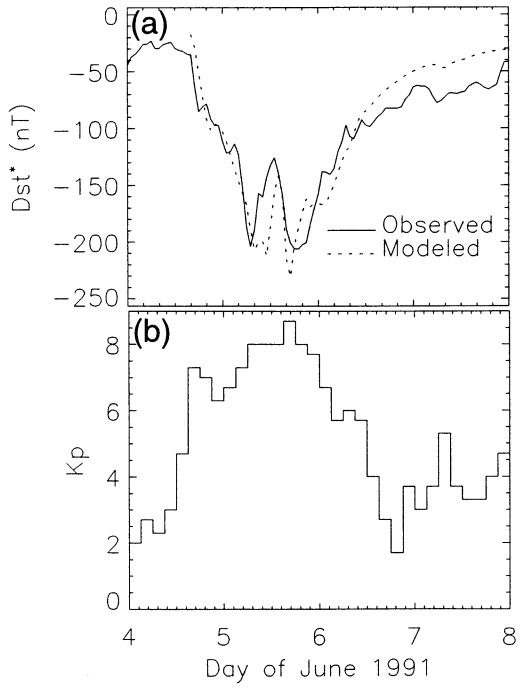

Figure 1. (a) Observed and calculated *Dst** and (b) *Kp* for the June, 4-7, 1991 geomagnetic storm.

3. Heat Input Into the Thermal Electrons

In order to tractably display the energy deposition rates, only the integrated quantity P_{iono} will be presented, as described in (5). This value can crudely be related back to the volume heating rate Q by dividing by the thickness (off-equatorial extent) of the ring current. This thickness varies from less than an Earth radius R_E to the entire half-length of the field line and can be quantified by the anisotropy of the ring current (that is, the ratio of the perpendicular and parallel pressures). Because this anisotropy is usually greater than 1, typical thicknesses extend over less than half of the equator-to-ionosphere distance.

Plate 1 shows P_{iono} (mapped to 800 km) at three times during the storm: at the initial *Dst* minimum during the main phase of the storm (0800 UT on June 5); during the fast recovery from the second *Dst* minimum of the storm (0000 UT on June 6); and well into the late-stage recovery of the storm (0000 on on June 8). Results are shown throughout the simulation domain, which spans all local times and magnetic latitudes from 40° to 65° (McIlwain L values of 2.0 to 6.5). These rates reach values over 10^{11} eV cm^{-2} s^{-1} on the duskside during the main phase of the storm and are still over 10^{10} eV cm^{-2} s^{-1} in the late recovery phase. These are very large heat fluxes, comparable to or larger than column heating rates from magnetospheric interaction of photoelectrons (maximum approximately 10^{11} on the dayside) and plasma sheet electrons (maximum approximately 10^9 on the nightside/dawnside) with the thermal electrons [*Khazanov et al.*, 1998, 2000]. While the heating rates given by *Khazanov et al.* [1998, 2000] are also at solar maximum, the geomagnetic activity was considerably different (that is, less intense), and thus it is not surprising that this heat flux is larger. There is strong local time asymmetry in the heating, and the peak is located toward lower latitudes near dusk. This is in agreement with the location of the maximum heating simulated by *Jordanova et al.* [1999]. Note that the peak shifts during the late stages, eventually moving toward higher latitudes. This is because the inner magnetosphere is being depleted of ring current particles while the outer regions of the simulation domain are still being supplied from the nightside boundary. The late-stage low-latitude values are an order of magnitude lower than what they were during the storm main phase, while the higher latitude values are essentially the same throughout.

Vertical slices through the results presented in Plate 1 are shown in Figure 2. The local time asymmetry of the heating is very clear in Figure 2 during the main phase of the storm (Figures 2a and 2b), but this asymmetry is removed by the late recovery phase (Figure 2c). Note that a sawtooth structure is evident in the results of Figure 2. This is a numerical artifact

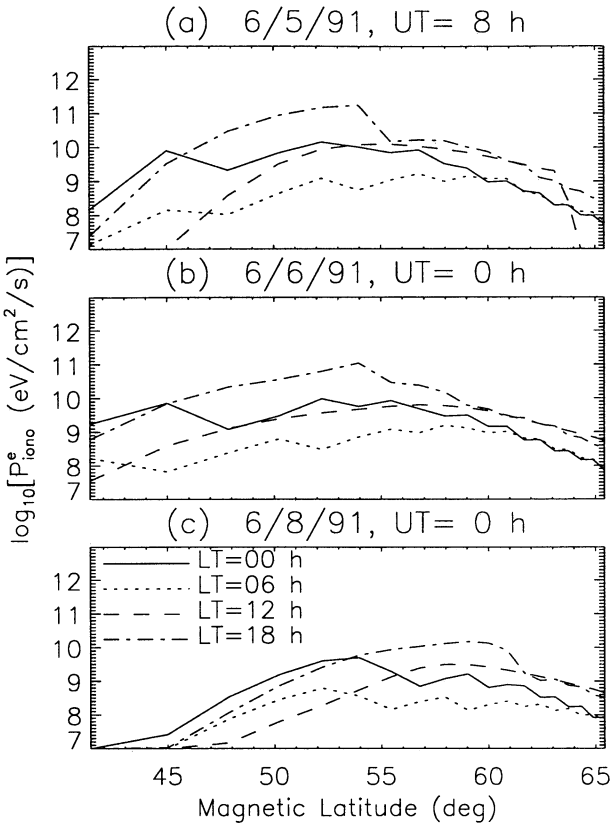

Figure 2. Line plots of the energy deposition rates shown in Plate 1 (a) at the first peak of the storm, (b) during the early recovery, and (c) well into the recovery stage.

resulting from the thermal plasma density model used in the simulations [those of *Rasmussen et al.*, 1993], which produces a stairstep radial density profile beyond the plasmapause. The presence of this numerical feature, however, does not change the main result of this study.

The local time asymmetry in the heating as a function of local time has two sources. The first is the asymmetry of the ring current, as the plasma sheet ions westwardly propagate through near-Earth space (the partial ring current). The ring current asymmetry is strongest during the main phase of the storm, when the convection strength rapidly drives the particles through the inner magnetosphere. The other reason for the local time asymmetry in the heating rates is the asymmetry in the thermal plasma density. Because P_{iono} is directly proportional to this quantity, thermal density structures such as the dusk bulge greatly influence the level of energy deposition. By the late recovery stage (Plate 1c and Figure 2c), the modeled ring current is nearly symmetric, and most of the asymmetry in P_{iono} is due to the thermal plasma structure.

The time development of the ionospheric heat input from the ring current heating of the thermal electrons is shown in Figure 3. The entire storm interval is presented for various spatial locations, specifically, magnetic latitudes corresponding to $L = 3$ and $L = 4$ (52° and 58° latitude, respectively), magnetic local time (MLT) 1800 and 2100 (four points on the duskside near the ring current-plasmasphere overlap), and also at the heating rate peak, wherever that occurs within the simulation domain. The peak heat input is seen to closely follow the $L = 3$ dusk line during the main phase of the storm and is usually above 10^{11} during this time. Later in the recovery phase, the peak shifts closer to evening $L = 4$, and the value never exceeds 10^{11}. These time series can be used to map the results of Plate 1 and Figure 2 throughout the storm interval. In order for the heating to reach such a high level, the ring current must overlap the dense plasmasphere. Even more importantly, however, the ions must have energies that allow them to interact efficiently with the thermal electrons. That is, for optimal energy transfer the ring current must be protons of a few keV in energy and/or oxygen ions in the tens of keV energy range. This simulation shows that the latter is occurring. Plasma sheet ions of a few keV have transported into the inner magnetosphere, adiabatically gaining energy up to the 30-70 keV energy range. In fact, the peak of the ring current O^+ distribution function is very near 50 keV, providing maximal heating to the thermal electrons, which were assumed to have a temperature of 1 eV everywhere.

4. Upper Ionospheric Consequences

To examine what effects these heat fluxes will have on the upper ionosphere, it is useful to compare the ring current model energy deposition rates with thermal plasma calculations from the field line interhemispheric plasma (FLIP) model, developed over the last 20 years [*Young et al.*, 1980; *Richards et al.*, 1983, 1998; *Torr et al.*, 1990]. Among many other things, this model calculates the thermal plasma temperature profile from various calculated or imposed magnetospheric heat sources. With the goal of quantifying the significance of the ring current heat inputs several simulations were conducted with this model for the magnetic field line above Millstone Hill Observatory (geographic location 43°N, 289°E) during the June 4-7, 1991, geomagnetic storm. In the first simulation run the topside ionospheric thermal electron temperature was forced to follow the observed electron temperature (at 604 km altitude), and the corresponding magnetospheric heat flux necessary to obtain such a temperature was calculated. So, within the assumptions of the FLIP model, this is a ground truth energy deposition rate, and its value during the storm should be a combination of the various heat sources.

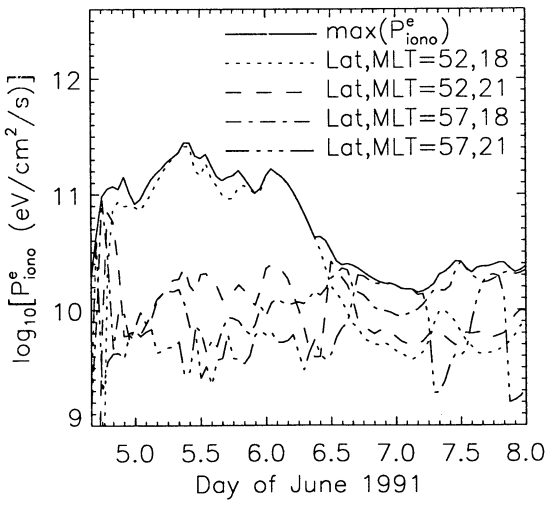

Figure 3. Energy deposition rates to the thermal electrons as a function of time throughout the June 1991 storm at several locations (and at the maximum, wherever that is located).

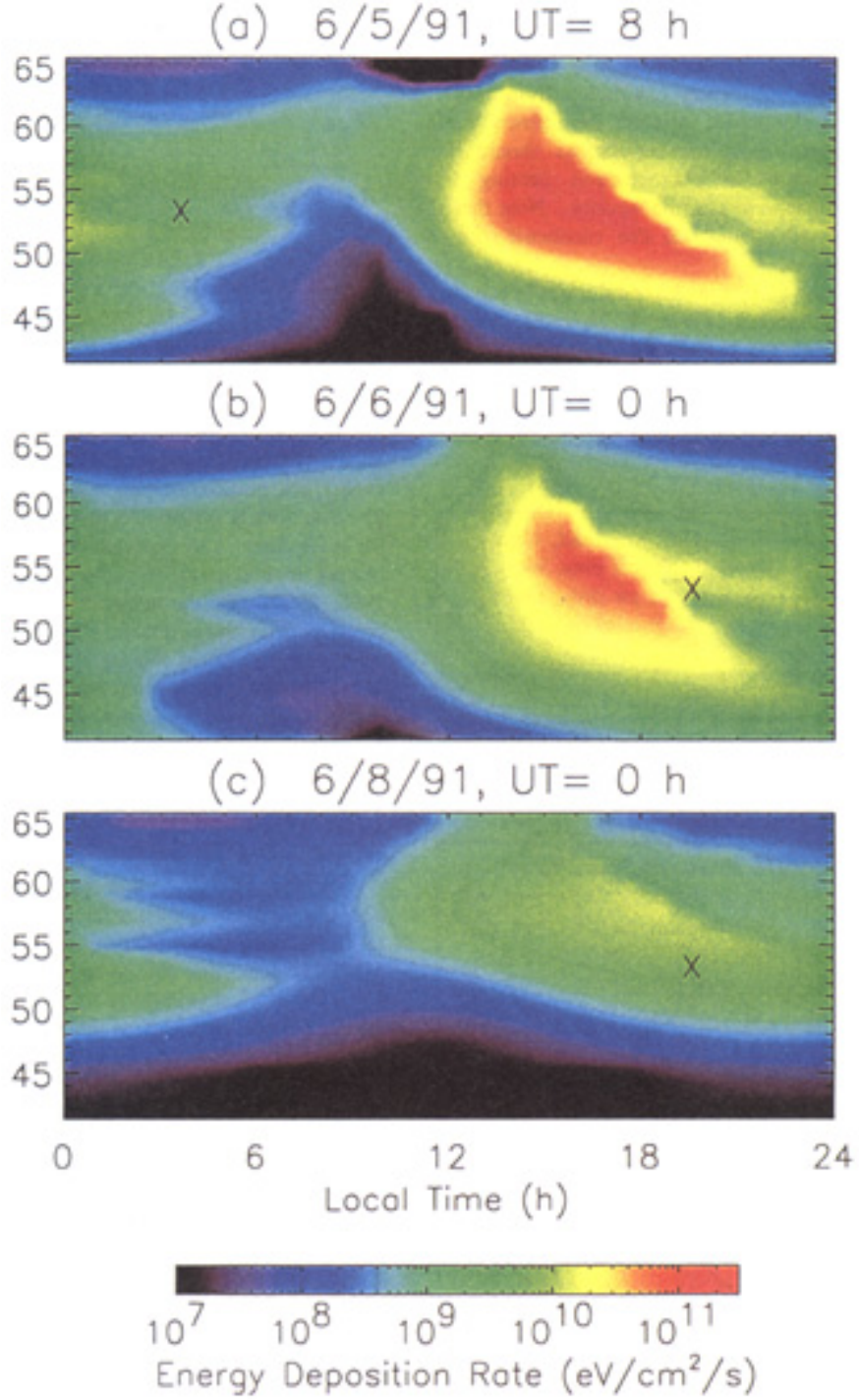

Plate 1. Modeled energy deposition rates (integrated along the field line, mapped to the topside ionosphere) from the ring current into the thermal electrons during the June 1991 storm (a) at the first peak of the storm, (b) during the early recovery, and (c) well into the recovery stage. Note the logarithmic scales. The black cross on each plot is the location of the Millstone Hill field line.

In the second and third simulations the magnetospheric heat flux was determined by the FLIP model using its photoelectron results, and the topside electron temperature was calculated using this number (note that only a photoelectron magnetospheric heat source was included, hereafter referred to as "pe only" simulations). These two solutions are for high and low thermal plasma density in the magnetosphere (the equatorial plane density for the high density run decays from 1500 to 800 cm^{-3} during the simulation, and the low density run is ~200 cm^{-3} throughout). These two simulations should show the difference that results in photoelectron heating from changing the magnetospheric electron density. Note that the imposed temperature calculation was also conducted with the high-density parameters.

Results from the ring current model and the FLIP code simulations are shown in Figure 4. Figure 4a shows the magnetospheric heat fluxes into the topside ionosphere above Millstone Hill calculated in the three runs. The electron temperature at 604 km altitude for the various FLIP simulations as well as the observed value are presented in Figure 4b. In addition, Figure 4c indicates the local time of these results during the event. The purpose of Figure 4a is to interpret the solid line (the heat flux to obtain the observed temperature) in terms of the other lines. As expected during the daylight hours, the heating is dominated by photoelectrons [cf. *Khazanov et al.*, 1998, 2000]. On the nightside, however, the photoelectron heat source is not sufficient. This is also seen in the middle panel of Figure 4b, as the calculated topside electron temperature from the photoelectron heat source is well below the observed temperature. It is not surprising that the heat inputs and temperatures from the two photoelectron FLIP runs are so close (less than a factor of 2 difference throughout most of the simulation). Most of the heat exchange for photoelectrons occurs near the ionosphere, where the thermal plasma densities are not that different.

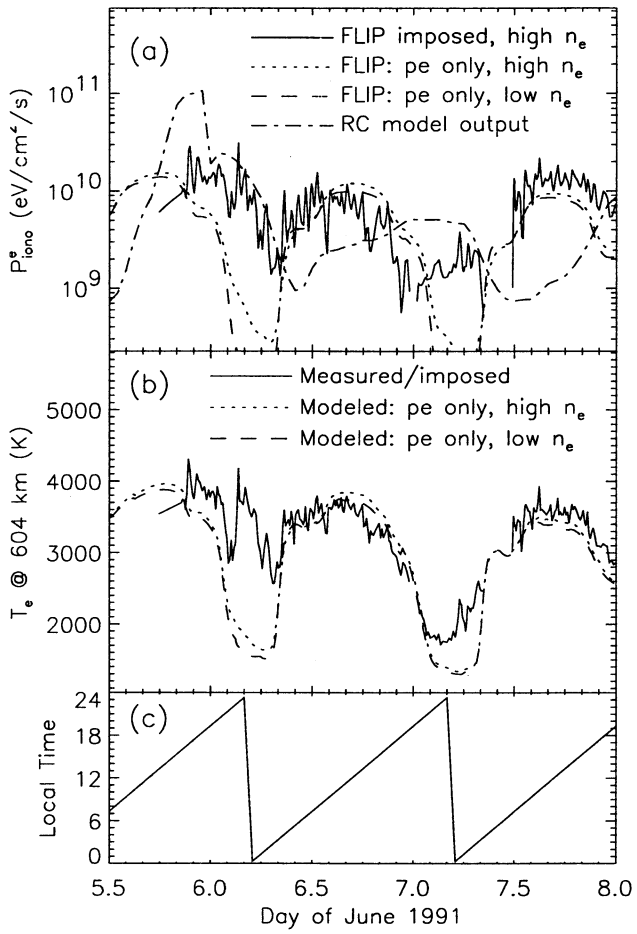

Figure 4. (a) Comparison of P_{iono} from the ring current simulation and from the FLIP model for the Millstone Hill field line during the storm. The first FLIP result is the heat input required to match the observed topside electron temperature, and the next two FLIP results are the heat inputs produced by photoelectrons for high and low plasmaspheric electron densities, respectively. (b) The observed topside temperature and the calculated temperature from the two FLIP results. (c) The local time of this field line.

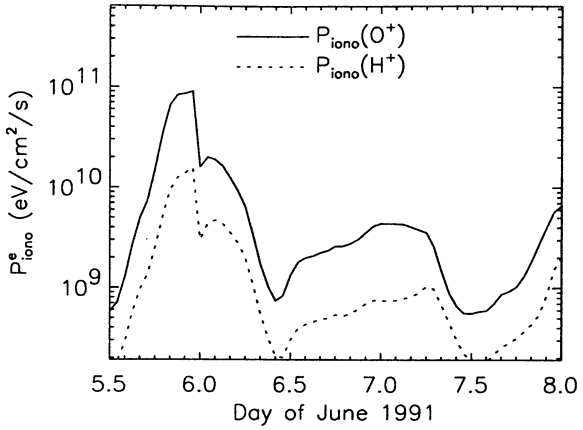

Figure 5. Energy deposition rates to the thermal electrons along the Millstone Hill field line during the June 1991 storm from the ring current H^+ and O^+ components.

It is seen in Figure 4a that the ring current heat flux is more than adequate to account for the observed heat input at the local times when photoelectrons are insufficient. Late on June 5, the calculated ring current energy deposition rate climbed to 10^{11} eV cm^{-2} s^{-1}, approaching an order of magnitude more than the FLIP model indicates as the necessary heat input. In the early hours of June 6, however, the ring current heating dropped down to coincide with the needed heating rate, and the comparison is quite good. During the next night the needed heat flux plummets to around $2x10^9$ eV cm^{-2} s^{-1}, which is slightly below the calculated ring current heat input. As before, though, the comparison gets better throughout the night, and the values are quite close at postmidnight local times. Reasons for these differences are discussed in section 5, but in spite of the caveats given there, it is clear that the ring current model reasonably predicts the necessary heating on the nightside, and so it can be said that the ring current is the dominant heat input to the thermal plasma on the nightside during storms at solar maximum. As mentioned in section 3, the reason for this is the abundance of oxygen ions in the tens of keV energy range. This is evidenced in Figure 5, which presents the heat input to the thermal electrons from the ring current H^+ and O^+ components along the Millstone Hill field line during the storm. It is seen that O^+ dominates the heating into the thermal electrons at this location (in fact, throughout the simulation range). Note that these high heating rates are only possible during solar maximum when a large O^+ population is present in the ring current.

It is interesting to examine what these heating rates mean in terms of upper ionospheric electron temperature and SAR arc emission rates. *Kozyra et al.* [1990] performed a comprehensive analysis of these relationships between incoming heat flux and temperature and emissions. It was found that for June during solar maximum the heat fluxes must reach 10^{10} eV cm^{-2} s^{-1} in order to even begin to create a SAR arc. This high threshold level (more than an order of magnitude higher than solar minimum) is because of the enhanced cooling rate during these times, as governed by changes to the neutral and ion particle composition and temperatures. However, *Kozyra et al.* [1990] showed that a heat input of 10^{11} eV cm^{-2} s^{-1} during this time (June at solar maximum) should yield topside electron temperatures near 5000 K and a 630 nm column emission rate of 4000 R. Keep in mind that this peak level of energy deposition is not achieved everywhere, but rather only on a small patch of the globe in the dusk sector near 52° magnetic latitude. Furthermore, it is unclear where the ionospheric density trough is located throughout this storm, and this peak heat input may not have been collocated with it. Therefore an estimation of SAR arc emission rates from these heat fluxes using the *Kozyra et al.* [1990] study results is not straightforward.

From *Buonsanto* [1995] and *Pavlov et al.* [1999] it appears that there was an ionospheric (*F* peak) density trough and temperature enhancement over Millstone Hill at approximately 2300 local time on June 5, 1991 (corresponding to 0400 UT on June 6). As seen in Figure 4, the calculated magnetospheric heat flux into the topside ionosphere was between $2\text{x}10^{10}$ and $3\text{x}10^{10}$ eV cm^{-2} s^{-1} from both the ring current model and the imposed temperature calculation. Using the summer solar maximum results of *Kozyra et al.* [1990], this heating rate range equates to a column SAR arc emission between 15 and 150 R. While emission observations are unavailable for this time period, these values indicate that there probably was not a SAR arc over Millstone Hill at this time. However, the intense heat input predicted by the model a few hours earlier would produce a 3000 R column emission [cf. *Kozyra et al.*, 1990], so there could have been a SAR arc over Millstone Hill at some point during the storm. Also, examination of Plate 1 (and similar plots throughout the storm) shows that the calculated extent of heat inputs from the ring current that are larger than 10^{10} is greater than 6 hours of MLT near 50° magnetic latitude during the peak of the storm. This is comparable to other observations of SAR arc extents during solar maximum [see, e.g., *Craven et al.*, 1982; *Kozyra et al.*, 1997].

5. Discussion

Let us now discuss some of the reasons for discrepancies between the ring current and FLIP simulation results. An obvious reason is the difference in the amount of thermal plasma along the field line between the two calculations. Figure 6 shows the equatorial plane thermal plasma densities that correspond to the line plots of Figure 2. Note that these values were mapped along the field line assuming that $n_e \propto B$ in the ring current simulations (needed for the Coulomb interactions with the ring current). At $L = 3$, the density ranges from 30 to 800 cm^{-3} during the main phase of the storm (when the field line is located inside and outside of the plasmapause) and has recovered to a nearly constant with local time value of 800 cm^{-3} by the late phase of the storm recovery (always in the plasmasphere). These values are not much different from the densities used in the FLIP model. However, unlike photoelectron heating where the energetic particles decrease in intensity with altitude, the majority of ring current heating occurs near the equator where the ring current is strongest. Therefore this inconsistency between the two simulations still could be a major factor in the differences between their solutions. If the real density was actually less than that calculated by the *Rasmussen et al.* [1993] model, then the comparison would be closer with the FLIP results. However, predicting the thermal plasma density in the magnetosphere is not a simple task, and it is even harder to predict the ring current-plasmasphere overlap where the heating is most intense. This aspect of the calculation will be much improved with a self-consistent ring current-thermal plasma model.

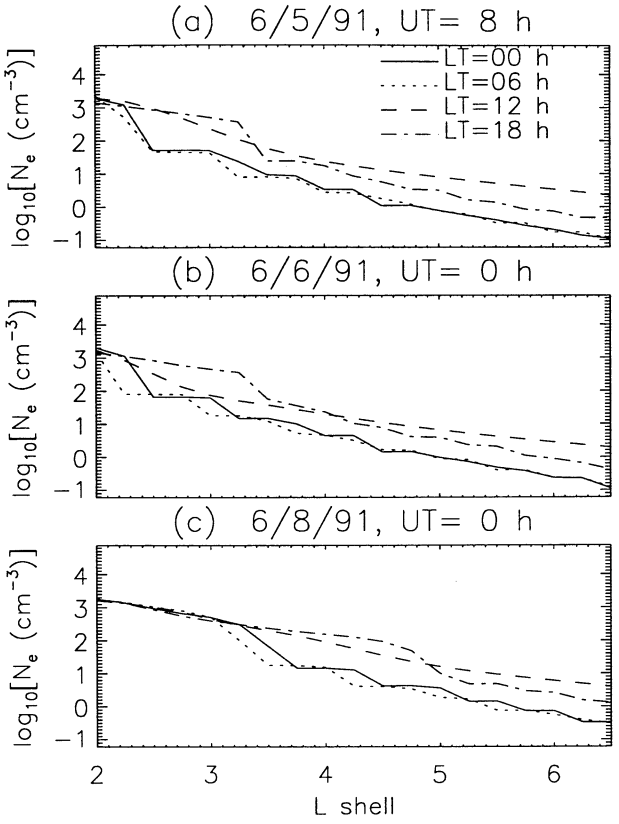

Figure 6. Thermal plasma density in the equatorial plane from the *Rasmussen et al.* [1993] model at the two times highlighted in this study during the June 1991 storm.

Note in Figure 6 the asymmetry in the density profiles throughout the storm. Even in the late recovery stage (Figure 6c), there is an order of magnitude more plasma at noon and dusk than at midnight and dawn. This asymmetry is responsible for a large part of the asymmetry seen in the energy deposition rates in Plate 1 and Figure 2. However, the thermal plasma asymmetry is not wholly responsible for the heating rate asymmetry observed during the main phase of the storm (compare Figures 2b and 2c), where ring current asymmetry is also responsible for the calculated dawn-dusk difference in energy deposition.

Another factor that could also be responsible for the differences in the energy deposition rates is that the thermal electron temperatures are different. The FLIP model calculates a temperature between 2000 and 5000 K throughout the storm,

while the ring current simulations assumed a constant 1 eV (11,600 K) electron temperature for the Coulomb interactions in this simulation. While this will not cause a large difference, a lower thermal electron temperature means that lower energy ring current ions will be the most efficient and transferring energy to the thermal electrons. This would cause a slight reduction in both the H^+ and O^+ heating rates and would reduce the energy deposition from the ring current (that is, help the comparison). Again, this will be improved with a self-consistent simulation that includes a thermal plasma temperature calculation.

Another reason is that the thermal plasma might not have a Maxwellian velocity space distribution. Because of the enhanced magnetospheric convection and large heat inputs during geomagnetic storms the distributions could be altered from their equilibrium shape. However, both the ring current model and the FLIP model assume that the thermal plasma has a Maxwellian shape. This variation would cause differences in the thermal plasma heating rates, as seen in other studies of energetic-thermal particle interactions [e.g., *Liemohn et al.*, 1999a]. Also, both energy deposition rate calculations assume instantaneous heat conduction along the field line. While this is not a bad assumption for electrons, conductivity issues have been raised about thermal ions [*Comfort et al.*, 1995a, 1995b], and delays in conduction would alter the time profile of the topside heating and temperature.

Yet another caveat is that the calculated ring current distribution may be different from the real particle distribution. The two primary factors in determining the ring current intensity in the inner magnetosphere are the density of the source population and the strength of the magnetospheric convection. The source population is taken from an extrapolation of LANL geosynchronous orbit data in both time and space to create a boundary condition for the entire nightside injection region. The convection strength is found from the Volland-Stern electric field model, driven by *Kp*. Both factors are sources of error in the ring current simulation [cf. *Kozyra et al.*, 1998; *Jordanova et al.*, 1999], and further study and improvements of these drivers are being conducted. In fact, a simulation using the statistical fits of *Borovsky et al.* [1998] for the nightside boundary conditions was conducted, and results of this are shown in Figure 7. Figure 7a shows that the *Dst** value is dramatically underestimated by the inflow of this source population, and Figure 7b shows that the heating rate is also substantially less than that found by the FLIP run with an imposed topside ionospheric electron temperature. This is an interesting result, because it indicates that the strength of the plasma sheet must be well known in order to obtain a reasonable result. The statistical fit does not reproduce the large density enhancements that occasionally impinge on the inner magnetosphere during the storm, and these missing bursts of high-intensity injection are largely responsible for the differences between the two simulations (since the convection field and the composition ratios were identical between the calculations).

Another ring current distribution error is introduced through the Coulomb interactions by the inconsistencies in the thermal plasma distribution with reality and also with other thermal plasma simulations (as discussed above).

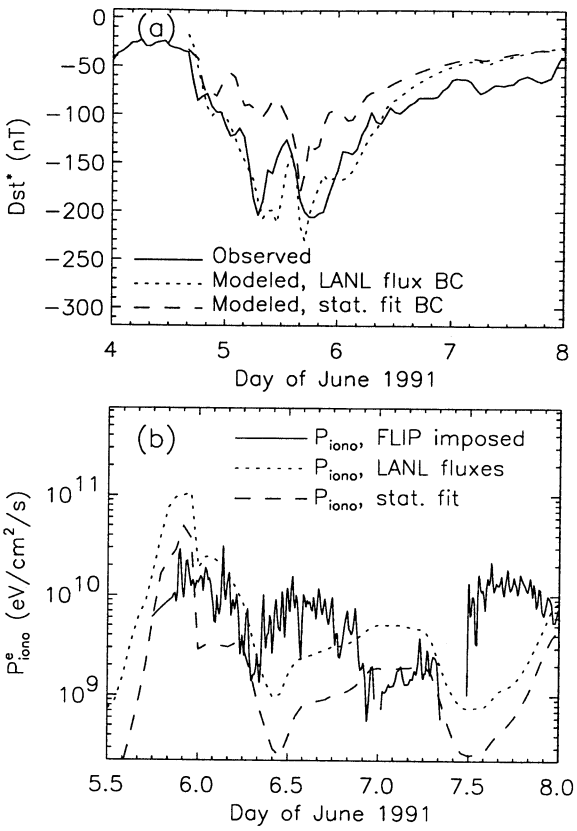

Figure 7. Comparison of results from the simulation discussed throughout the text (LANL flux boundary condition (BC)) and another simulation with a statistical fit boundary condition. Shown are (a) *Dst** for each run along with the observed value and (b) P_{iono} for each run, along with the FLIP result for an imposed electron temperature.

6. Conclusion

The heating from the ring current ions to the thermal plasma during a major geomagnetic storm at solar maximum has been presented and examined, along with some of the consequences of such heating. The storm of June 4-7, 1991, was chosen for this study because of the large set of studies already focusing on this event. These results are meant to complement the existing literature and provide a guide to the development of global ionospheric and magnetospheric thermal particle models and observations.

For the heat input to the thermal electrons from the ring current the intense heating rates calculated by these simulations will have substantial consequences on the upper ionosphere and thermosphere. In addition to heating the thermal electrons in this region and exciting atomic oxygen it will also influence the atmospheric density, temperature, and composition. At these altitudes, energy transfer to the thermal ions is also more efficient than in the magnetosphere, and so the upper ionospheric ion temperature will be elevated because of this heat input. This will have ramifications for the magnetospheric ion temperature calculation, as the temperature at the ionospheric foot point of the field lines rises and falls with this energy source. Such a phenomenon was seen over Millstone Hill during this storm, and results from the FLIP model were compared with the heating rates from the ring current simulations. It was concluded that photoelectrons were still a major dayside heat source at this location (L = 3) during the storm, but that the ring current heat input is necessary (and, in fact, fully adequate) to match the elevated topside temperatures on the nightside during the storm.

In spite of the caveats listed above in comparing the ring current simulation results with the FLIP simulation results, it is clear that very large energy deposition rates to the thermal electrons are possible during geomagnetic storms at solar maximum. The highest heating rates occur where the ring current and plasmasphere overlap, as expected. However, the results of this study indicate that it is the presence of the O^+ component, which is greatly enhanced at solar maximum, that is responsible for these large heating rates and that the ring current heat source is fully adequate to cause the observed topside ionospheric electron temperatures on the nightside.

Acknowledgments. The authors would like to thank Michelle Thomsen and Joe Borovsky for providing the LANL data for the ring current simulation boundary conditions. This work was supported by National Science Foundation (NSF) grants ATM-9711381, ATM-9710326, ATM-9815108, and ATM-9800830 and National Aeronautics and Space Administration (NASA) grants NCC8-181, NAG-4771, and NAG5-6976. Support for this research was also provided by a Research Seed Grant from the Michigan Space Grant Consortium.

Janet G. Luhmann thanks Margaret W. Chen and another referee for their assistance in evaluating this paper.

References

Arriagada, M. A., A. J. Foppiano, and M. J. Buonsanto, Horizontal meridional winds over King George Island, Antarctica, during the June 1991 geomagnetic storm, *J. Atmos. Sol.-Terr. Phys., 60*, 1007-1012, 1998.

Bittencourt, J. A., *Fundamentals of Plasma Physics*, Pergamon, Tarrytown, N. Y., 1986.

Borovsky, J. E., M. F. Thomsen, and R. C. Elphic, The driving of the plasma sheet by the solar wind, *J. Geophys. Res., 103*, 17,617-17,639, 1998.

Buonsanto, M. J., Millstone Hill incoherent scatter *F*-region observations during the disturbances of June 1991, *J. Geophys. Res., 100*, 5743-5755, 1995.

Burke, W. J., N. C. Maynard, M. P. Hagan, R. A. Wolf, G. R. Wilson, L. C. Gentile, M. S. Gussenhoven, C. Y. Huang, T. W. Garner, and F. J. Rich, Electrodynamics of the inner magnetosphere observed in the dusk sector by CRRES and DMSP during the magnetic storm of June 4 - 6, 1991, *J. Geophys. Res., 103*, 29,399-29,418, 1998.

Burton, R. K., R. L. McPherron, and C. T. Russell, An empirical relationship between interplanetary conditions and *Dst*, *J. Geophys. Res., 80*, 4204-4214, 1975.

Chandler, M. O., J. U. Kozyra, J. L. Horwitz, R. H. Comfort, and L. H. Brace, Modeling of the thermal plasma in the outer plasmasphere: A magnetospheric heat source, in *Modeling Magnetospheric Plasma, Geophys. Monogr. Ser.*, vol. 44, edited by T. E. Moore and J. H. Waite Jr., pp. 101-105, AGU, Washington, D. C., 1988.

Comfort, R. H., P. G. Richards, P. D. Craven, and M. O. Chandler, Problems in simulating ion temperatures in low density flux tubes, in *Cross-Scale Coupling in Space Plasmas, Geophys. Monogr. Ser.*, vol. 93, edited by J. L. Horwitz, N. Singh, and J. L. Burch J. L., pp. 155-160, AGU, Washington, D. C., 1995a.

Comfort, R. H., P. D. Craven, and P. G. Richards, A modified thermal conductivity for low density plasma magnetic flux tubes, *Geophys. Res. Lett., 22*, 2457-2460, 1995b.

Craven, J. D., L. A. Frank, and K. L. Ackerson, Global observations of a SAR arc, *Geophys. Res. Lett., 9*, 961-964, 1982.

Daglis, I. A., The role of magnetosphere-ionosphere coupling in magnetic storm dynamics, in *Magnetic Storms, Geophys. Monogr. Ser.*, vol. 98, edited by B. T. Tsurutani, W. D. Gonzalez, Y. Kamide, and J. K. Arballo, pp. 107-116, AGU, Washington, D. C., 1997.

Daglis, I. A., E. T. Sarris, and B. Wilken, AMPTE/CCE observations of the ion population at geosynchronous altitudes, *Ann. Geophys., 11*, 685-696, 1993.

Dessler, A. J., and E. N. Parker, Hydromagnetic theory of geomagnetic storms, *J. Geophys. Res., 64*, 2239-2252, 1959.

Fok, M.-C., J. U. Kozyra, and L. H. Brace, Solar cycle variation in the subauroral electron temperature enhancement: Comparison of AE-C and DE 2 satellite observations, *J. Geophys. Res., 96*, 1861-1866, 1991.

Fok, M.-C., J. U. Kozyra, A. F. Nagy, C. E. Rasmussen, and G. V. Khazanov, Decay of equatorial ring current ions and associated aeronomical consequences, *J. Geophys. Res., 98*, 19,381-19,393, 1993.

Fok, M.-C., P. D. Craven, T. E. Moore, P. G. Richards, Ring current-plasmasphere coupling through Coulomb collisions,in *Cross-Scale Coupling in Space Plasmas, Geophys. Monogr. Ser.*, vol. 93, edited by J. L. Horwitz, N. Singh, and J. L. Burch J. L., pp. 161-171, AGU, Washington, D. C., 1995.

Hudson, M. K., S. R. Elkington, J. G. Lyon, V. A. Marchenko, I. Roth, M. Temerin, J. B. Blake, M. S. Gussenhoven, and J. R. Wygant, Simulations of radiation belt formation during storm sudden commencements, *J. Geophys. Res., 102*, 14,087-14,102, 1997.

Jordanova, V. K., L. M. Kistler, J. U. Kozyra, G. V. Khazanov, and A. F. Nagy, Collisional losses of ring current ions, *J. Geophys. Res., 101*, 111-126, 1996.

Jordanova, V. K., R. B. Torbert, R. M. Thorne, H. L. Collin, J. L. Roeder, and J. C. Foster, Ring current activity during the early $Bz<0$ phase of the January 1997 magnetic cloud, *J. Geophys. Res., 104*, 24,895-24,914, 1999.

Khazanov, G. V., M. W. Liemohn, J. U. Kozyra, and T. E. Moore, Inner magnetospheric superthermal electron transport: Photoelectron and plasma sheet electron sources, *J. Geophys. Res., 103*, 23,485-23,501, 1998.

Khazanov, G. V., M. W. Liemohn, J. U. Kozyra, and D. L. Gallagher, Global energy deposition to the topside ionosphere from superthermal electrons, *J. Atmos. Sol.-Terr. Phys.*, in press, 2000.

Kozyra, J. U., Magnetic storm effects in the inner magnetosphere: The decay of the Earth's ring current, *Phys. Space Plasmas, 12*, 185-222, 1992.

Kozyra, J. U., and A. F. Nagy, Ring current decay - Coupling of ring current energy into the thermosphere/ionosphere system, *J. Geomagn. Geoelectr., 43*, suppl., 285-295, 1991.

Kozyra, J. U., E. G. Shelley, R. H. Comfort, L. H. Brace, T. E. Cravens, and A. F. Nagy, The role of ring current O^+ in the formation of stable auroral red arcs, *J. Geophys. Res., 92*, 7487-7502, 1987.

Kozyra, J. U., C. E. Valladares, H. C. Carlson, M. J. Buonsanto, and D. W. Slater, A theoretical study of the seasonal and solar cycle variations of stable auroral red arcs, *J. Geophys. Res., 95*, 12,219-12,234, 1990.

Kozyra, J. U., M. O. Chandler, D. C. Hamilton, W. K. Peterson, D. M. Klumpar, D. W. Slater, M. J. Buonsanto, and H. C. Carlson, The role of ring current nose events in producing stable auroral red arc intensifications during the main phase: Observations during the September 19-24, 1984, equinox transition study, *J. Geophys. Res., 98*, 9267-9283, 1993.

Kozyra, J. U., A. F. Nagy, and D. W. Slater, High-altitude energy source(s) for stable auroral red arcs, *Rev. Geophys., 35*, 155-190, 1997.

Kozyra, J. U., V. K. Jordanova, J. E. Borovsky, M. F. Thomsen, D. J. Knipp, D. S. Evans, D. J. McComas, and T. E. Cayton, Effects of a high-density plasma sheet on ring current development during the November 2-6, 1993, magnetic storm, *J. Geophys. Res., 103*, 26,285-26,305, 1998.

Liemohn, M. W., G. V. Khazanov, P. D. Craven, and J. U. Kozyra, Nonlinear kinetic modeling of early stage plasmaspheric refilling, *J. Geophys. Res., 104*, 10,295-10,306, 1999a.

Liemohn, M. W., J. U. Kozyra, V. K. Jordanova, G. V. Khazanov, M. F. Thomsen, and T. E. Cayton, Analysis of early phase ring current recovery mechanisms during geomagnetic storms, *Geophys. Res. Lett., 26*, 2845-2849, 1999b.

Lobzin, V. V., and A. V. Pavlov, Correlations between SAR arc intensity and solar and geomagnetic activity, *Ann. Geophys., 17*, 770-781, 1999.

Mihalov, J. D., and R. J. Strangeway, Large solar wind disturbances during late May and early June 1991, *Sol. Phys., 160*, 363-370, 1995.

Ogunade, S. O., Solar activity and interplanetary disturbances, *Astrophys. Space Sci., 258*, 35-46, 1997.

Pavlov, A. V., M. J. Buonsanto, A. C. Schleiser, and P. G. Richards, Comparison of models and data at Millstone Hill during the 5-11 June 1991 storm, *J. Atmos. Sol.-Terr. Phys., 61*, 263-279, 1999.

Rasmussen, C. E., S. M. Guiter, and S. G. Thomas, Two-dimensional model of the plasmasphere: refilling time constants, *Planet. Space Sci., 41*, 35-42, 1993.

Rees, M. H., and R. G. Roble, Observations and theory of the formation of stable auroral red arcs, *Rev. Geophys., 13*, 201-242, 1975.

Richards, P. G., R. W. Schunk, and J. J. Sojka, Large-scale counter-

streaming of H^+ and He^+ along plasmaspheric flux tubes, *J. Geophys. Res.*, *88*, 7879-7886, 1983.

Richards, P. G., P. L. Dyson, T. P. Davies, M. L. Parkinson, and A. J. Reeves, Behavior of the ionosphere and thermosphere at a southern mid-latitude station during magnetic storms in early March 1995, *J. Geophys. Res.*, *103*, 26,421-26,432, 1998.

Roeder, J. L., J. F. Fennell, M. W. Chen, M. Grande, S. Livi, and M. Schulz, CRRES observations of stormtime ring current ion composition, in *Workshop on the Earth's Trapped Particle Environment*, *AIP Conf. Proc., 383*, edited by G. D. Reeves, 131-143, 1996.

Salah, J. E., W. Deng, and R. R. Clark, Observed response of the earth's lower thermosphere to a major geomagnetic storm, *Geophys. Res. Lett., 23*, 575-578, 1996.

Scali, J. L., and B. W. Reinisch, Geomagnetic storm time studies using Digisonde data, *Adv. Space Res., 20*(9), 1679-1688, 1997.

Sckopke, N., A general relation between the energy of trapped particles and the disturbance field near the earth, *J. Geophys. Res.*, *71*, 3125-3130, 1966.

Shue, J.-H., et al., Magnetopause location under extreme solar wind conditions, *J. Geophys. Res.*, *103*, 17,691-17,700, 1998.

Smart, D. F., and M. A. Shea, Solar-interplanetary circumstances associated with the major events in March and June 1991 and comparison with similar events of previous solar cycles, *Adv. Space Res., 17*(2), 147-150, 1995.

Smith, R. W., G. Hernandez, K. Price, G. Fraser, K. C. Clark, W. J. Schulz, S. Smith, and M. Clark, The June 1991 thermospheric storm observed in the southern hemisphere, *J. Geophys. Res.*, *99*, 17,609-17,615, 1994.

Torr, M. R., D. G. Torr, P. G. Richards, and S. P. Yung, Mid- and low-latitude model of thermospheric emissions, 1, $O^+(2P)$ 7320 Å and N2(2P) 3371 Å, *J. Geophys. Res.*, *95*, 21,147-21,168, 1990.

Usmanov, A. V., and M. Dryer, A global 3-D simulation of interplanetary dynamics in June 1991, *Sol. Phys., 159*, 347-370, 1995.

Young, D. T., H. Balsiger, and J. Geiss, Correlations of magnetospheric ion composition with geomagnetic and solar activity, *J. Geophys. Res., 87*, 9077-9096, 1982.

Young, E. R., P. G. Richards, and D. G. Torr, A flux preserving method of coupling first and second order equations to simulate the flow of plasma between the protonosphere and the ionosphere, *Comput. Phys., 38*, 141-156, 1980.

V. K. Jordanova, Space Science Center, University of New Hampshire, 408 Mose Hall, Durham, NH 03824-3525. (vania.jordanova@unh.edu)

G. V. Khazanov, Geophysical Institute and Department of Physics, University of Alaska Fairbanks, 903 Koyukuk Drive, P. O. Box 757320, Fairbanks, AK 99775-7320. (khazanov@gi.alaska.edu)

J. U. Kozyra and M. W. Liemohn, Space Physics Research Laboratory, University of Michigan, 2455 Hayward Street, Ann arbor, MI 48109-2143. (jukozyra@umich.edu; liemohn@umich.edu)

P. G. Richards, Computer Science Department, University of Alabama in Huntsville, Huntsville, AL 35806. (richards@cs.uah.edu)

(Received March 14, 2000; revised May 9, 2000;
accepted June 5, 2000.)